Investigation of bamboo pulp fiber-reinforced unsaturated polyester composites

Citation	Qiu, R., Liu, W., & Li, K. 2015. Investigation of bamboo pulp fiber-reinforced unsaturated polyester composites. Holzforschung, 69(8), 967-974. doi:10.1515/hf-2014-0207
DOI	10.1515/hf-2014-0207
Publisher	De Gruyter
Version	Version of Record
Terms of Use	http://cdss.library.oregonstate.edu/sa-termsofuse

Renhui Qiu, Wendi Liu and Kaichang Li*

Investigation of bamboo pulp fiber-reinforced unsaturated polyester composites

Abstract: Mechanical pulp fibers (MPFs) and chemical pulp fibers (CPFs) from moso bamboo have been characterized in terms of their length and width distributions, and their reinforcing effects in unsaturated polyester (UPE) composites have also been investigated. CPF-UPE composites had much higher tensile strength, flexural strength, and flexural modulus than MPF-UPE composites. CPF-UPE composites also absorbed less water than MPF-UPE composites. Treatments of the fibers with a combination of 1,6-diisocyanatohexane (DIH) and 2-hydroxyethyl acrylate (HEA) significantly increased the tensile strength, flexural strength, flexural modulus, and water resistance of the resulting composites. Fourier transform infrared and X-ray photoelectron spectroscopy analyses indicated that DIH-HEA was bound onto bamboo fibers (BFs) via carbamate linkages. The scanning electron microscopy images of the tensile-fractured surfaces of the composites revealed that the DIH-HEA treatments for BFs greatly improved the interfacial adhesion between the fibers and UPE resins.

Keywords: bamboo fibers, interfacial adhesion, mechanical properties, surface treatments, unsaturated polyester, water resistance

DOI 10.1515/hf-2014-0207
Received July 15, 2014; accepted November 14, 2014; previously published online December 17, 2014

Introduction

Glass fiber-reinforced unsaturated polyester (UPE) composites are widely used in marine structures, automobiles, home construction, sporting goods, and furniture. However, the production of glass fibers is energy consuming. Inhalable carcinogenic fine particles are typically generated in the production of glass fiber-reinforced UPE composites. Plant fibers from hemp (*Cannabis sativa*), flax (*Linum usitatissimum*), kenaf (*Hibiscus cannabinus*), jute (*Corchorus capsularis*), sisal (*Agave sisalana*), banana (*Musa paradisiaca*), and agave (*Agave americana*) have been studied for the replacement of glass fibers in such composites (Pothan et al. 2006; Bessadok et al. 2008; Demir et al. 2011; Prasad and Rao 2011; Bozaci et al. 2013; Khalil et al. 2013; Sawpan et al. 2013). Bamboo, especially moso bamboo (*Phyllostachys heterocycla* cv. *pubescens*), is abundant and readily available in China. Moso bamboo fibers (BFs) have high specific stiffness and are inexpensive (Yu et al. 2011). BFs were prepared by steam explosion, alkali treatment, and chemical degumming; their effects on the mechanical properties and water absorption in BF-UPE composites were investigated (Kim et al. 2013). BFs were obtained from the removal of lignin by NaOH treatment followed by a combination of compression molding and roller milling and then used for the preparation and characterization of unidirectional BF-polyester composites (Deshpande et al. 2000). BFs were also prepared by the treatment of bamboo strips in NaOH solution via crushing by a hydraulic press, boiling in water in a pressure cooker, and manual separation of the fibers. The resulting fibers were used in combination with glass fibers for the preparation of hybrid UPE composites (Mandal and Alam 2012). BFs were also obtained through soaking of bamboo strips in water for 3 days followed by gentle beating, scrapping with a sharp-edged knife, and combing, and the fibers were tested as reinforcing materials in UPE composites (Rao et al. 2010; Prasad and Rao 2011). Manually decorticated bamboo fibrous strips were prepared from a chemical degumming of the culm-containing tissues and used as reinforcement in UPE composites (Prasad and Rao 2011). It is well known that the chemical composition, distribution of fiber lengths and widths, and length-to-width ratio depend on the preparation processes and have great impacts on the properties of BF-UPE composites. However, data about the characteristics of BFs are mainly limited to single fiber characteristics (Yang et al. 2009; Yu et al. 2011; Wang et al. 2014) or the chemical analysis of bamboo tissues and BFs (Sun

***Corresponding author: Kaichang Li,** Department of Wood Science and Engineering, Oregon State University, Corvallis, OR 97331, USA, Phone: +1-541-737 8421, Fax: +1-541-737 3385, e-mail: kaichang.li@oregonstate.edu
Renhui Qiu: College of Material Engineering, Fujian Agriculture and Forestry University, Fuzhou 350002, P.R. China; and Department of Wood Science and Engineering, Oregon State University, Corvallis, OR 97331, USA
Wendi Liu: College of Material Engineering, Fujian Agriculture and Forestry University, Fuzhou 350002, P.R. China

et al. 2011; Qu et al. 2012; Vena et al. 2013). Data concerning fiber length and fiber width distribution are difficult to find in the literature.

Bamboo is commonly used for the production of composite panels, furniture, and houses as well as for paper production. In China, chemical pulp (CP) from bamboo is produced by the kraft process, and stone-ground pulping is a typical process for the production of mechanical pulp (MP). Wood pulp fibers were tested as reinforcing materials in UPE (Du et al. 2012, 2013), but these fibers are different from bamboo pulp fibers in terms of fiber strengths, shapes, and chemical composition (Hammett et al. 2001; Yang et al. 2008; Zhao et al. 2010; Chaowana 2013). Both CP and MP from bamboo are readily available in a large quantity and are fairly inexpensive. Such fibers, however, were not investigated as reinforcing materials in UPE composites. In this study, both CP fibers (CPFs) and MP fibers (MPFs) were characterized in terms of fiber lengths, fiber widths, and the aspect ratios. The performance of both fiber types was tested in UPE composites. Another goal of the present study was to modify the fibers with a combination of 1,6-diisocyanatohexane (DIH) and 2-hydroxyethyl acrylate (HEA) as a coupling agent for the further improvement of the mechanical properties and water resistance of the resulting BF-UPE composites.

Materials and methods

Sources of materials: bamboo (*Phyllostachys pubescens*) MP boards (Minghua Fiber Board, Youxi, Fujian, China); bamboo CP boards (Zhongzhu Pulp and Paper, Shaowu, Fujian, China); Aropol 7030 (a mixture of 60% UPE and 40% styrene) and LP-4016 [poly(vinyl acetate)] (Ashland Chemical, Columbus, OH, USA); styrene, *tert*-butyl peroxybenzoate (TBPB), and DIH (Sigma-Aldrich, Milwaukee, WI, USA); zinc stearate (Acros Organics, Morris Plains, NJ, USA); HEA (TCI America, Portland, OR, USA); and anhydrous ethyl acetate (EMD Chemicals, Inc., Gibbstown, NJ, USA).

MP boards and CP boards (80 g) were cut into pieces (40×40 mm) and then soaked into distilled water (1500 ml) for 4 h at room temperature (r.t.). The water-saturated pulp board pieces were separated into individual fibers with a pulp disintegrator for 10 min, and the wet pulp mat (200×200 mm) was prepared in a paper handsheet former and oven-dried at 103°C for 24 h. The oven-dried mats were kept in sealed plastic bags at r.t. before use.

Aropol 7030 resins (910 g) and LP-4016 (420 g) resins were mixed together, styrene (70 g) and zinc stearate (63 g) were then added to the solution, and the resulting mixture was mechanically stirred at r.t. for 2 h to form UPE resins. The composition of UPE resins was 62.2% Aropol 7030 resins, 28.6% LP-4016 resins, 4.8% styrene, and 4.4% zinc stearate.

The fiber distribution was analyzed with a Morfi Compact fiber analyzer (Techpap, Inc., Grenoble, Cedex, France). The oven-dried boards (0.03 g) were soaked in distilled water (1000 ml) for 4 h at r.t., treated in a pulp disintegrator for 10 min, and poured into a 1000 ml cup for fiber analysis. The consistency of the fiber suspension in the cup was 0.003%. The cup with the fiber suspension was placed on the No. 1 position of the analyzer, and another empty 1000 ml cup was placed on the position of W as the receiving container. The testing parameters were set as follows: 5000 for number of fibers, 200 μm for the minimum fiber length, and 10 000 μm for the maximum fiber length. After the analyzer was turned on, the suction tube of the analyzer was put into the fiber suspension cup, allowing the aqueous fibrous suspension to flow through a cell for the measurement of fibers. The fiber length and fiber width of each individual fiber were measured, recorded, and evaluated.

The cellulose content of fibers was determined by nitric acid and ethanol extraction based on TAPPI T201 wd-76. The pentosan content was determined by titration in accordance with TAPPI T223 cm-01. The Klason lignin content of fibers was measured in accordance with TAPPI T222 om-11.

DIH (2.40 g, 14.28 mmol) and HEA (1.65 g, 14.28 mmol) were dissolved in anhydrous ethyl acetate (70 ml). The DIH usage was 3% based on the dry weight of BFs, and the HEA/DIH molar ratio was kept at 1:1. The mixture was magnetically stirred at r.t. for 10 min. The resulting solution was evenly sprayed onto the surfaces of the oven-dried MPF or CPF mats (80 g) with a spray bottle. The resulting DIH-HEA-coated fiber mats were then oven dried at 50°C for 5 h before composite preparation.

For the preparation of BF-UPE composites with 50% fiber loading, UPE resins (80 g) and TBPB (0.80 g) were mixed by a spatula for 1 min. The mixture was evenly poured onto the surfaces of MPF or CPF mats (80 g). Subsequently, the mat was placed in a stainless steel mold with a cavity dimension of 200×200×3 mm. The hot-press conditions from Qiu et al. (2011) were adopted. The mold was first pressed in a bench-top Carver press (Carver, Inc., Wabash, IN, USA) at r.t. and at 3.24 MPa for 5 min. The hot pressing continued at 3.24 MPa for 10 min at 110°C. The press platens were further heated to 160°C, at which the mold was pressed at 4.24 MPa for 30 min. When the hot pressing was finished, the mold was removed from the press and cooled at r.t.

Dumbbell specimens with the narrow section of 50.0×10.0×3.0 mm were prepared from rectangular specimens (80.0×15.0×3.0 mm) and were used for the evaluation of tensile strength of the composites based on ASTM D3039-08. The rectangular specimens (60×12.7×3.0 mm) were tested for the flexural properties of the composites based on ASTM D790-10. The tests were conducted with a Sintech machine (MTS Systems, Enumclaw, WA, USA) at a crosshead speed of 5 mm min^{-1}.

The water absorption of BF-UPE composites was measured by soaking the composite specimens in distilled water at r.t. in accordance with ASTM D5229. The composite boards were cut into bars (76.2×25.4 mm) for water uptake measurement. All specimens were first conditioned in an oven at 50°C for 24 h, cooled in a desiccator to r.t., weighed, and then immediately soaked in water. At a predetermined time, the specimens were removed from water, wiped with tissue paper, measured for its weight gain, and then put back into water for continued soaking. The water uptake percentage was determined as the weight gain divided by the dry weight of the specimen.

The scanning electron microscopy (SEM) images of the fractured surfaces of the tensile-test specimens were obtained by a FEI Quanta 600 SEM (Hillsboro, OR, USA). The tensile-fractured specimens were frozen by liquid nitrogen and cut into 2- to 3-mm-long samples, whereas the original tensile-fractured surface was maintained. The

fractured surfaces were coated with an Au-Pd film (8–10 nm) before testing. The SEM images had an imaging resolution of 4 nm, and the dimensions of the view field were 145×130 μm with ×1000 magnification. The accelerating voltage of SEM was 10.0 kV.

The untreated CPFs (CPF_{untr}) (5 g) and DIH-HEA-treated CPFs (CPF_{tr}) (5 g) were first wrapped into a piece of filter paper and then extracted with chloroform at 70°C in a Soxhlet extractor for 24 h. After oven drying at 103°C for 24 h, the extracted samples were powdered for the characterization with Fourier transform infrared (FTIR) and X-ray photoelectron spectroscopy (XPS). The FTIR spectra were obtained on a Nexus 470 FTIR spectrometer (Thermo Nicolet, Madison, WI, USA). The XPS experiments were conducted with an ESCALAB 250 X-ray photoelectron spectrometer (Thermo Fisher Scientific, Waltham, MA, USA). The testing parameters were the vacuum of 2×10^{-10} mbar and spot size at 500 μm with Al Kα source.

The mechanical properties data and water uptake data were compared with one-way ANOVA with GraphPad Prism 3.0 (GraphPad Software, La Jolla, CA, USA). All comparisons were conducted based on a 95% confidence interval.

Results and discussion

Characteristics and chemical compositions of BFs

The arithmetical average fiber length and the weighted average fiber length of CPFs and MPFs were similar (Table 1). The same was true for the average width. The coarseness of MPFs was much higher than that of CPFs, indicating that each individual CPF was much lighter than each individual MPF.

Macrofibrils had diameters of <1.0 μm in the fiber wall (Paiva et al. 2007). MPFs had a higher percentage of macrofibrils in length than CPFs (Table 1). The maximum length of fines was generally defined to be 0.2 mm (Meyers and Nanko 2005). MPFs had a higher percentage of fines both in length and area than CPFs, which indicated that MPFs contained much more fines than CPFs (Table 1).

Fines with lengths smaller than 0.20 mm were not further analyzed. Fibers with lengths of 0.2–10 mm were analyzed for length and width distributions (Figure 1a and b). The length of all fibers was within the range of 0.20–3.52 mm (Figure 1a). About 75% of CPFs had lengths between 0.45 and 1.55 mm, whereas only 63% of MPFs were within this range (Figure 1a). The percentage of MPFs at the wider length range of 0.45–2.34 mm was 79%, which was comparable with the 75% of CPFs at the narrower range of 0.45–1.55 mm (Figure 1a). These results indicated that CPFs had narrower length distributions than MPFs. About 86% of CPFs had widths ranging from 11 to 46 μm, and about 88% of MPFs had widths at this range, which indicated that CPFs and MPFs had similar width distributions (Figure 1b). CPFs contained 92.4% cellulose, 11.2% pentosan, and no lignin, and MPFs contained 55.8% cellulose, 12.1% pentosan, and 19.9% Klason lignin.

Table 1 Characteristic of MPFs and CPFs.

Characteristics	MPFs	CPFs
Arithmetical average length (mm)[a]	0.748	0.657
Average weighted length by length (mm)[b]	1.091	0.901
Average width (μm)[c]	24.9	24.7
Coarseness (mg m^{-1})[d]	0.2615	0.0368
Macrofibrils in length (%)[e]	1.276	0.667
Fines in length (%)[f]	40.2	31.6
Fines in area (%)[g]	9.84	2.62

[a]The sum of the lengths of all individual fibers divided by the total number of fibers measured.
[b]The sum of individual fiber lengths squared divided by the sum of the individual fiber lengths.
[c]The sum of individual fiber width divided by the total number of fibers measured.
[d]The weight per unit length of fiber.
[e]The ratio of total fiber length to the sum of total fiber length and total macrofibril length (Huber et al. 2008).
[f]The total length of all measurable fines divided by the total length of all measurable fines and fibers.
[g]The total area of all measurable fines divided by the total area of all measurable fines and fibers.

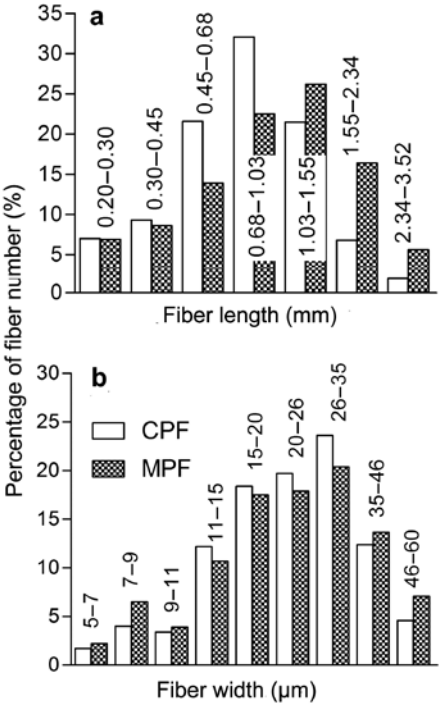

Figure 1 Percentages of fiber number in (a) length and (b) width.

Mechanical properties of CPF and MPF composites

The tensile strength of CPF_{untr}-UPE was 97.3% higher than that of MPF_{untr}-UPE, and the tensile strength of CPF_{tr}-UPE was 87.0% higher than that of MPF_{tr}-UPE (Figure 2a). The tensile strength of CPF_{tr}-UPE was 30.5% higher than that of CPF_{untr}-UPE, and the tensile strength of MPF_{tr}-UPE was 24.5% higher than that of MPF_{untr}-UPE (Figure 2a). The flexural strength and flexural modulus of CPF_{untr}-UPE were 101.1% and 53.4% higher than that of MPF_{untr}-UPE, respectively (Figure 2b). CPF_{tr}-UPE had 110.7% and 58.8% higher flexural strength and flexural modulus than MPF_{tr}-UPE, respectively (Figure 2b). The flexural strength of CPF_{tr}-UPE was 30.9% higher than that of CPF_{untr}-UPE, and the flexural strength of MPF_{tr}-UPE was 25.4% higher than that of MPF_{untr}-UPE. CPF_{tr}-UPE had 10.7% higher flexural modulus than CPF_{untr}-UPE. The flexural modulus of MPF_{tr}-UPE was 7.2% higher than that of MPF_{untr}-UPE.

The tensile strength, flexural strength, and flexural modulus of both CPF_{untr}-UPE and CPF_{tr}-UPE were much higher than those of MPF_{untr}-UPE and MPF_{tr}-UPE. Although CPFs and MPFs had comparable average length and average width, the coarseness of MPFs was much higher than that of CPFs, indicating that each individual CPF, on average, was much lighter and much more porous than each MPF. The high porosity of CPFs allowed UPE resins to better penetrate and impregnate CPFs than MPFs, which would enhance the reinforcing effects and thus enhance the mechanical properties of the composites. The number of CPFs with similar average lengths and widths was much more than that of MPFs on the same weight of fiber mats, which would allow CPF-UPE to have more fibers to withstand the same amount of stress transferred from the matrix than MPF-UPE. It has been known that fines in pulp fibers contributed much less on the reinforcing effects than fibers (Lin et al. 2007). The MPF mat had a much higher content of fines than the CPF mat, which partially explained why MPF-UPE had lower strengths and modulus than CPF-UPE. Additionally, CPFs had a much higher content of cellulose than MPFs. It has been demonstrated that the tensile strength and modulus of fibers increased with the increase in the cellulose content of the fibers (John and Thomas 2008). The high strengths of reinforcing fibers would definitely lead to high strengths and high modulus of the fiber-reinforced UPE composites, which explained why CPF-UPE composites were stronger than MPF-UPE composites. That the DIH-HEA treatment increased the tensile strength, flexural strength, and flexural modulus of the resulting BF-UPE composites can be due to the enhanced interfacial adhesion between the treated fibers and UPE reins.

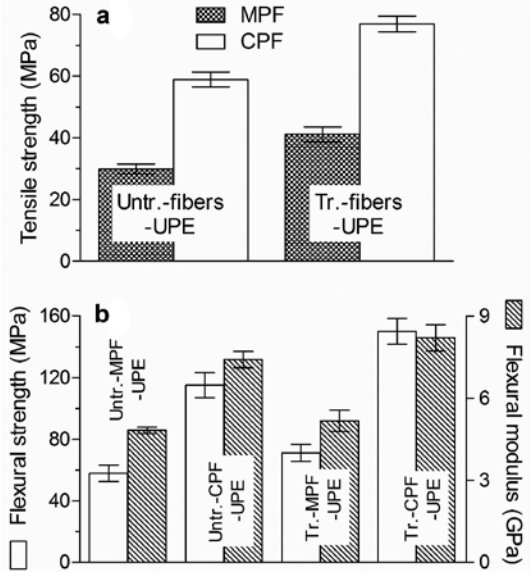

Figure 2 Mechanical properties of BF-UPE composites: (a) tensile strength and (b) flexural strength and flexural modulus.
Data are the means of five replicates of each group, and the error bars represent SD.

Water absorption of composites

The water uptake percentage of all composites increased with soaking time (Figure 3). The water absorption of MPF_{untr}-UPE reached equilibrium moisture content (EMC) at approximately 40 days of soaking, whereas, for CPF_{untr}-UPE, 20 days of soaking were sufficient to reach EMC. MPF_{tr}-UPE reached EMC after 80 days, whereas 40 days were enough for CPF_{tr}-UPE to reach EMC. The water uptake percentage of MPF_{untr}-UPE at EMC was higher than that of

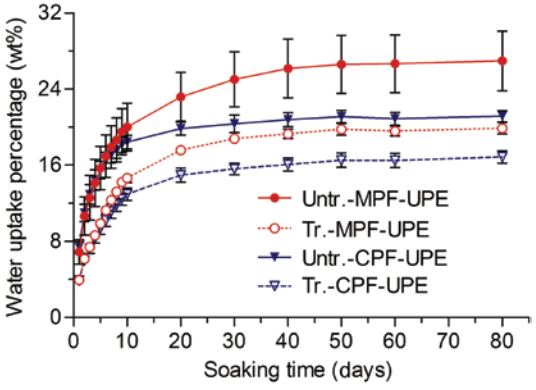

Figure 3 Water uptake percentages of BF-UPE composites.

CPF_{untr}-UPE. MPF_{tr}-UPE also had a higher water uptake percentage than CPF_{tr}-UPE at their EMC points. The water uptake percentages of both MPF-UPE and CPF-UPE composites significantly decreased at their EMC points after DIH-HEA treatment.

Several studies showed that the water absorption of hemp or BF-reinforced composites made of UPE, polyethylene, or polypropylene followed the Fick's law; that is, the water absorption percentages at the early stage of soaking at r.t. conformed to Equation (1) (Espert et al. 2004; Kushwaha and Kumar 2011; Chen et al. 2013; Fang et al. 2013). Thus, the initial linear segment of water uptake data (at the first week of soaking) of MPF-UPE and CPF-UPE were analyzed with regression against Equation (1):

$$M_t / M_m = kt^n \quad (1)$$

where M_t is the water uptake percentage at time t, M_m is the water uptake percentage at the equilibrium, k and n are constants that represent the characteristics of water diffusion taking place inside the composites, k shows the interaction intensity between composites and water molecules, and n indicates the behavior of water absorption in the composites. That values of R^2 were at least 0.97 in Table 2 implied that the water uptake data fitted Equation (1) well. The diffusion coefficient (D), which represents the velocity of water molecules moving inside the composites, was calculated with Equation (2) (Sreekumar et al. 2009):

$$D = \pi[(kh)/(4M_m)]^2 \quad (2)$$

where h is the initial thickness of specimen and k is the slope of the initial linear part of the water uptake data.

The calculated diffusion parameters of CPF-UPE and MPF-UPE composites are listed in Table 2. All n values in Table 2 were close to 0.5, indicating that the behavior of the water absorption basically fitted the Fickian model; that is, the water molecules moved from the outside to the inside region of composites with a gradient of water concentration (Kushwaha and Kumar 2011). When the EMC inside the composites was reached, it remained stable throughout the soaking time (Kushwaha and Kumar 2011). Although the M_m of MPF_{untr}-UPE was much higher than that of CPF_{untr}-UPE, CPF_{untr}-UPE had higher k and D values than those of MPF_{untr}-UPE (Table 2). A similar tendency of the M_m, k, and D values occurred between MPF_{tr}-UPE and CPF_{tr}-UPE. As discussed previously, UPE resins could better penetrate and impregnate CPFs than MPFs and thus formed a better coverage of CPF surfaces with UPE resins and better interfacial adhesion between UPE resins and CPFs. The better coverage and the better interfacial adhesion would reduce the amount of hydroxyl groups available for the absorption of water, which explained why CPF-UPE had a lower M_m than MPF-UPE. However, CPFs had less lignin coverage on the cellulose surfaces and had more porosity, making the water molecules contact directly with cellulose of CPFs. This is beneficial for water molecules moving into the composites at a higher velocity, resulting in higher k and D values of CPF-UPE composites than those of MPF-UPE composites.

The fiber treatment significantly decreased the k values of both CPF-UPE and MPF-UPE (Table 2), indicating weaker interactions between water molecules and the treated BF-UPE. Both CPF-UPE and MPF-UPE had decreased M_m and D values after fiber treatment (Table 2). The reactions of the hydroxyl groups on the surfaces of BFs with the isocyanate groups of DIH reduced the hydrophilicity of the fibers. The stronger interface of the composites after fiber treatment decreased the availability of the gaps between fibers and matrices for water penetration, thus reducing the M_m, k, and D values of both MPF_{tr}-UPE and CPF_{tr}-UPE.

Analyses of FTIR and XPS of CPFs

Compared with the FTIR spectrum of CPF_{untr}, the spectrum of CPF_{tr} displayed three new peaks: (1) a strong C=O peak at 1720 cm^{-1}, (2) a N-H peak at 1535 cm^{-1}, and (3) a C-N peak at 1252 cm^{-1} (Figure 4). All these new peaks illustrated the existence of carbamates that resulted from the reactions between the isocyanate groups of DIH and the hydroxyl groups of CPFs or HEA in CPF_{tr}. A separate experiment has demonstrated that DIH, HEA, and the reaction products

Table 2 Diffusion parameters of UPE composites prepared with DIH-HEA-treated and untreated MPF and CPF fibers.

Samples	n	k (h^{-n})	h (mm)	R^2	EWU[a] (M_m) (%)	Diffusion coefficient (D)×10^{-13} (m^2 s^{-1})
MPF_{untr}-UPE	0.482	0.058	3.325	0.987	26.97	20.18
CPF_{untr}-UPE	0.428	0.094	3.098	0.978	21.15	46.69
MPF_{tr}-UPE	0.574	0.026	3.312	0.995	17.51	3.96
CPF_{tr}-UPE	0.527	0.038	3.196	0.998	15.27	8.25

[a]Equilibrium water uptake.

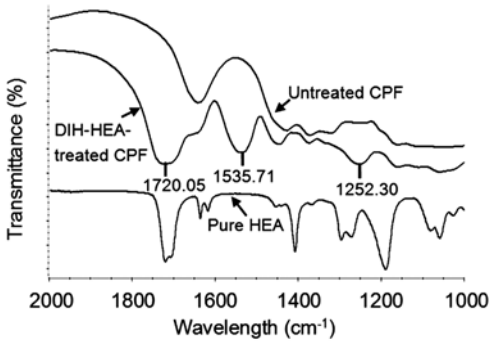

Figure 4 FTIR spectra of HEA and chloroform-extracted CPF with and without DIH-HEA treatment.

of DIH and HEA were soluble in chloroform. Therefore, any residual DIH and HEA and any reaction products of DIH and HEA that were not covalently bonded onto CPFs should have been removed by chloroform extraction. The carbamates were thus covalently linked with CPFs.

The analysis of CPFs with high-resolution XPS provided the concentrations of covalent bonds and functional groups on the surfaces of CPFs (Table 3). Both CPF_{untr} and CPF_{tr} showed characteristic covalent bonds and functional groups (C-C/C-H, C-O, C=O/O-C-O, and O-C=O) on the surfaces of cellulosic fibers (Johansson and Campbell 2004). After the treatment of CPFs with DIH-HEA, new C-N and N-C=O groups, although at relatively low content of about 3.5%, appeared on the fiber surfaces, which confirmed the existence of new N-containing functional groups such as carbamates (Table 3). Furthermore, the increase in the content of O-C=O group from 5.2% to 6.5% suggested more ester groups, such as the ester group of HEA that had been bounded onto the fiber surfaces after CPFs were treated with DIH-HEA.

The DIH/HEA molar ratio was kept at 1:1 throughout this study; that is, the molar ratio of isocyanate groups of DIH to the hydroxyl group of HEA was 2:1. Thus, the excessive isocyanate groups in the DIH-HEA solution were expected to react with the hydroxyl groups on the surfaces of fibers. The pending C=C bonds in the treated fibers were expected to form covalent linkages with the matrix during the free radical polymerization of UPE resins. Furthermore, there were more hydroxyl groups available for the reactions on CPF surfaces than on MPF surfaces, which may explain why the chemical treatment was more effective for CPFs than MPFs and resulted in higher gains of the tensile strength, flexural strength, and flexural modulus of CPF-UPE than MPF-UPE.

Table 3 Concentrations of functional groups (%) on the surface of CPFs from the high-resolution C1s peak of XPS.

Functional groups	CPF_{untr} (%)	CPF_{tr} (%)
C-C/C-H	24.44	24.05
C-OH/C-O-C	55.52	49.48
C=O/O-C-O	14.78	12.98
O-C=O	5.24	6.52
C-N	–	3.46
N-C=O	–	3.52

Interfacial adhesion of composites

The separation between fibers and resins and fiber pullout were clearly visible in the SEM images of the fractured surface of MPF_{untr}-UPE composites (Figure 5a). The SEM images of CPF_{untr}-UPE composites showed that individual fibers were embedded into the matrix, and several fibers were torn apart (Figure 5b). The results from Figure 5a and b indicated that the interfacial adhesion between fibers and the UPE matrix was better for CPF_{untr}-UPE than for MPF_{untr}-UPE. Similarly, individual fibers with clean surfaces were still observed from the SEM image of MPF_{tr}-UPE composites (Figure 5c), whereas the SEM image of CPF_{tr}-UPE composites showed that some fibers were defibrillated, and less single fibers could be observed on the fractured surface (Figure 5d), indicating a better interfacial adhesion between fibers and the UPE matrix for CPF_{tr}-UPE than for MPF_{tr}-UPE.

Conclusions

CPFs and MPFs have similar arithmetical average fiber length, weighted average fiber length, and average width. MPFs have much higher coarseness, percentages of macrofibrils in length, and percentage of fines both in length and area compared to CPFs. CPFs have narrower length distributions than MPFs, but their width distributions are similar to that of MPFs. CPFs contain more cellulose than MPFs, but the pentosan contents of both fibers are similar. CPF-UPE composites have much higher tensile strength, flexural strength, and flexural modulus and lower water uptake at equilibrium than MPF-UPE composites. The water uptake of both composites follows basically the Fick's law. Treatments of CPFs and MPFs with DIH-HEA significantly improve the tensile strength, flexural strength, and flexural modulus and significantly reduce the water uptake of the resulting composites.

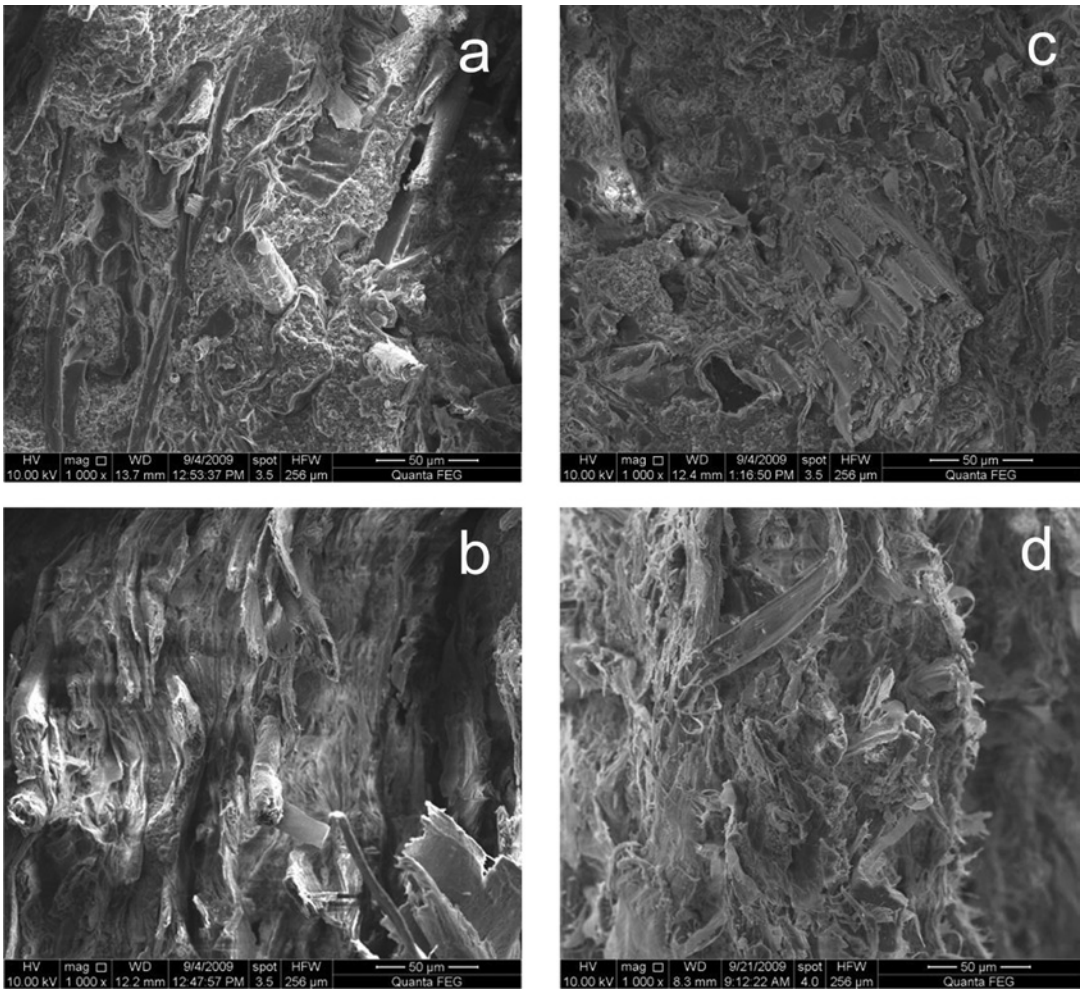

Figure 5 SEM images of tensile-fractured surface of composites: (a) untreated MPF-UPE, (b) treated MPF-UPE, (c) untreated CPF-UPE, and (d) treated CPF-UPE.

Acknowledgments: This research was supported by grants to R.Q. from the National Natural Science Foundation of China (Grant No. 31070495), the Fujian Provincial Funding for Cooperative Project of Higher Education Institutions and Industries, China (Grant No. 2013H6005), and the China Ministry of Education for the Doctoral Programs in Higher Education Institutions (Grant No. 20133515110015).

References

Bessadok, A., Marais, S., Roudesli, S., Lixon, C., Métayer, M. (2008) Influence of chemical modifications on water-sorption and mechanical properties of Agave fibres. Composites Part A 39:29–45.

Bozaci, E., Sever, K., Sarikanat, M., Seki, Y., Demir, A., Ozdogan, E., Tavman, I. (2013) Effects of the atmospheric plasma treatments on surface and mechanical properties of flax fiber and adhesion between fiber-matrix for composite materials. Composites Part B 45:565–572.

Chaowana, P. (2013) Bamboo: an alternative raw material for wood and wood-based composites. J. Mater. Sci. Res. 2:91–102.

Chen, T., Liu, W., Qiu, R. (2013) Mechanical properties and water absorption of hemp fibers reinforced unsaturated polyester composites: effect of fiber surface treatment with a heterofunctional monomer. BioResources 8:2780–2791.

Demir, A., Seki, Y., Bozaci, E., Sarikanat, M., Erden, S., Sever, K., Ozdogan, E. (2011) Effect of the atmospheric plasma treatment parameters on jute fabric: the effect on mechanical properties of jute fabric/polyester composites. J. Appl. Polym. Sci. 121:634–638.

Deshpande, A.P., Bhaskar Rao, M., Lakshmana Rao, C. (2000) Extraction of bamboo fibers and their use as reinforcement in polymeric composites. J. Appl. Polym. Sci. 76:83–92.

Du, Y., Yan, N., Kortschot, M.T. (2012) Investigation of unsaturated polyester composites reinforced by aspen high-yield pulp fibers. Polym. Compos. 33:169–177.

Du, Y., Wu, T., Yan, N., Kortschot, M.T., Farnood, R. (2013) Pulp fiber-reinforced thermoset polymer composites: effects of the pulp fibers and polymer. Composites Part B 48:10–17.

Espert, A., Vilaplana, F., Karlsson, S. (2004) Comparison of water absorption in natural cellulosic fibers from wood and one year crops in polypropylene composites and its influence on their mechanical properties. Composites Part A 35:1267–1276.

Fang, H., Zhang, Y., Deng, J., Rodrigue, D. (2013) Effect of fiber treatment on the water absorption and mechanical properties of hemp fiber/polyethylene composites. J. Appl. Polym. Sci. 127:942–949.

Hammett, A.L., Youngs, R.L., Sun, X., Chandra, M. (2001) Non-wood fiber as an alternative to wood fiber in China's pulp and paper industry. Holzforschung 55:219–224.

Huber, P., Carré, B., Petit-Conil, M. (2008) The influence of TMP fibre flexibility on flocculation and formation. BioResources 3:1218–1227.

Johansson, L.S., Campbell, J.M. (2004) Reproducible XPS on biopolymers: cellulose studies. Surf. Interf. Anal. 36: 1018–1022.

John, M.J., Thomas, S. (2008) Biofibres and biocomposites. Carbohydr. Polym. 71:343–364.

Khalil, H.A., Suraya, N., Atiqah, N., Jawaid, M., Hassan, A. (2013) Mechanical and thermal properties of chemical treated kenaf fibres reinforced polyester composites. J. Compos. Mater. 47:3343–3350.

Kim, H., Okubo, K., Fujii, T., Takemura K. (2013) Influence of fiber extraction and surface modification on mechanical properties of green composites with bamboo fiber. J. Adhes. Sci. Technol. 27:1348–1358.

Kushwaha, P.K., Kumar, R. (2011) Influence of chemical treatments on the mechanical and water absorption properties of bamboo fiber composites. J. Reinf. Plast. Compos. 30:73–85.

Lin, T., Yin, X., Retulainen, E., Nazhad, M.M. (2007) Effect of chemical pulp fines on filler retention and paper properties. Appita J. 60:469–473.

Mandal, S., Alam, S. (2012) Dynamic mechanical analysis and morphological studies of glass/bamboo fiber reinforced unsaturated polyester resin-based hybrid composites. J. Appl. Polym. Sci. 125:382–387.

Meyers, J., Nanko, H. (2005) Effects of fines on the fiber length and coarseness values measured by the fiber quality analyzer (FQA). Paper presented at the 2005 TAPPI Practical Papermaking Conference, Milwaukee, WI, USA, May 22–26, 2005.

Paiva, A.T., Sequeira, S.M., Evtuguin, D.V., Kholkin, A.L., Portugal I. (2007) Nanoscale structure of cellulosic materials: challenges and opportunities for AFM. In: Modern Research and Educational Topics in Microscopy. Eds. Méndez-Vilas, A., Díaz, J. Formatex Research Center, Badajoz, Spain. pp. 726–733.

Pothan, L.A., Thomas, S., Groeninckx, G. (2006) The role of fibre/matrix interactions on the dynamic mechanical properties of chemically modified banana fibre/polyester composites. Composites Part A 37:1260–1269.

Prasad, A.V.R., Rao, K.M. (2011) Mechanical properties of natural fibre reinforced polyester composites: Jowar, sisal and bamboo. Mater. Des. 32:4658–4663.

Qiu, R., Ren, X., Fifield, L.S., Simmons, K.L., Li, K. (2011) Hemp-fiber-reinforced unsaturated polyester composites: optimization of processing and improvement of interfacial adhesion. J. Appl. Polym. Sci. 121:862–868.

Qu, C., Kishimoto, T., Ogita, S., Hamada, M., Nakajima, N. (2012) Dissolution and acetylation of ball-milled birch (*Betula platyphylla*) and bamboo (*Phyllostachys nigra*) in the ionic liquid [Bmim]Cl for HSQC NMR analysis. Holzforschung 66:607–614.

Rao, K.M.M., Rao, K.M., Prasad, A.V.R. (2010) Fabrication and testing of natural fibre composites: Vakka, sisal, bamboo and banana. Mater. Des. 31:508–513.

Sawpan, M.A., Pickering, K.L., Fernyhough, A. (2013) Analysis of mechanical properties of hemp fibre reinforced unsaturated polyester composites. J. Compos. Mater. 47:1513–1525.

Sreekumar, P.A., Thomas, S.P., Saiter, J.M., Joseph, K., Unnikrishnan, G., Thomas, S. (2009) Effect of fiber surface modification on the mechanical and water absorption characteristics of sisal/polyester composites fabricated by resin transfer molding. Composites Part A 40:1777–1784.

Sun, B., Liu, J., Liu, S., Yang, Q. (2011) Application of FT-NIR-DR and FT-IR-ATR spectroscopy to estimate the chemical composition of bamboo (*Neosinocalamus affinis* Keng). Holzforschung 65:689–696.

Vena, P.F., Brienzo, M., del Prado G.-A.M., Görgens, J.F., Rypstra, T. (2013) Hemicelluloses extraction from giant bamboo (*Bambusa balcooa* Roxburgh) prior to kraft or soda-AQ pulping and its effect on pulp physical properties. Holzforschung 67:863–870.

Wang, H., An, X., Li, W., Wang, H., Yu, Y. (2014) Variation of mechanical properties of single bamboo fibers (*Dendrocalamus latiflorus* Munro) with respect to age and location in culms. Holzforschung 68:291–297.

Yang, Z., Xu, S., Ma, X., Wang, S. (2008) Characterization and acetylation behavior of bamboo pulp. Wood Sci. Technol. 42:621–632.

Yang, G., Zhang, Y., Shao, H., Hu, X. (2009) A comparative study of bamboo Lyocell fiber and other regenerated cellulose fibers. 2nd ICC 2007, Tokyo, Japan, October 25–29, 2007. Holzforschung 63:18–22.

Yu, Y., Tian, G., Wang, H., Fei, B., Wang, G. (2011) Mechanical characterization of single bamboo fibers with nanoindentation and microtensile technique. Holzforschung 65:113–119.

Zhao, G., Lai, R., He, B., Greschik, T., Li, X. (2010) Replacement of softwood kraft pulp with ECF-bleached bamboo kraft pulp in fine paper. BioResources 5:1733–1744.